Scientific Research Publishing

Open Journal of Applied Sciences, 2024, 14, 3441-3459
https://www.scirp.org/journal/ojapps
ISSN Online: 2165-3925
ISSN Print: 2165-3917

Structured Laser Illumination Planar Imaging (SLIPI): Separating the Absorption and Scattering Coefficients Using Kubelka-Munk Relationship

Serge Martial Adepo[1,2*], Jocelyne Mamaket Bosson[1], Guy-Oscar Regnima[2,3], Sylvere Bienvenue Dion[2], Thomas Koffi[2,4], Michel Kouacou Abaka[2], Thouakesseh Jérémie Zoueu[2]

[1]Laboratoire de Physique Fondamentale Appliquée (LPFA), Université Nangui Abrogoua, Unité de Formation et de Recherche des Sciences Fondamentales Appliquées, Abidjan, Côte d'Ivoire
[2]Laboratoire d'Instrumentation, Image et Spectroscopie (L2IS), Institut National Polytechnique Felix Houphouët-Boigny, Département de Formation et de Recherche du Génie Electrique et Electronique, Yamoussoukro, Côte d'Ivoire
[3]Unité de Formation et de Recherche en Sciences et Technologie, Département de Physique, Université de Man, Man, Côte d'Ivoire
[4]Ecoles d'Ingénieurs en Bâtiment et Travaux Publics (BTP) et Construction Navale (CN) Université Polytechnique de San-Pédro (UPSP), San Pedro, Côte d'Ivoire
Email: *sergeadepo65@gmail.com

How to cite this paper: Adepo, S.M., Bosson, J.M., Regnima, G.-O., Dion, S.B., Koffi, T., Abaka, M.K. and Zoueu, T.J. (2024) Structured Laser Illumination Planar Imaging (SLIPI): Separating the Absorption and Scattering Coefficients Using Kubelka-Munk Relationship. *Open Journal of Applied Sciences*, **14**, 3441-3459.
https://doi.org/10.4236/ojapps.2024.1412225

Received: November 4, 2024
Accepted: December 7, 2024
Published: December 10, 2024

Abstract

Determining the optical properties of media remains an important part of scientific research. Knowledge of these optical properties, particularly absorption and diffusion coefficients, has direct applications in biomedical therapeutic diagnostics. The determination of these coefficients was previously reserved for optically dilute media. Recently, a technique called Structured Laser Illumination Planar Imaging (SLIPI) has been developed for measuring extinction coefficients in dense media. For such a medium and technique, no study has reported the determination of absorption and scattering coefficients. In this study, we have developed a simple calculation method based on the combination of Kubelka-Munk relations and extinction, both functions of the medium's absorption and diffusion coefficients. The equations thus developed enable absorption and diffusion coefficients to be easily calculated from extinction coefficient measurements alone, using the SLIPI technique. The analysis method thus developed was applied to ten (10) milk solutions of different concentrations considered to be predominantly diffusive, and to ten (10) coffee solutions of different concentrations considered to be predominantly absorbent. The coefficient values obtained have been analysed and compared to the literature ones and they would be satisfactory.

Keywords

Structured Illumination, Extinction Coefficient, Absorption Coefficient, Scattering, Coefficient, Kubelka-Munk Coefficients

1. Introduction

Absorption and scattering are the main phenomena of light-matter interaction [1]. As such, the study of these phenomena is then used to characterize different environments. In the case of biological tissues, the extraction of such parameters allows for effective and safe medical therapy and diagnosis, enabling consistent monitoring of these tissues [2]-[4]. These properties can also be used to optimize light dose distribution during photodynamic therapy of cancer cells [5]-[7], as well as to differentiate healthy tissue from diseased tissue. For instance, it has been shown that an Alzheimer's patient's brain presents a low absorption coefficient but a significantly high reduced scattering coefficient [8]. Similarly, an infected burn area is distinguishable from a non-infected one due to its relatively high absorption coefficient and low reduced scattering coefficient [9].

These optical properties are typically determined using various non-invasive techniques, which are recurrent techniques utilizing continuous wave sources in combination with fluence measurements [10] [11]. Other researchers have developed a modulated imaging technique based on structured illumination [12]. For example, [13] describes an optical imaging system with structured illumination and integrated detection, based on the Kubelka-Munk (K-M) propagation model, for spatial characterization of absorption and scattering properties in turbid media.

Recently, Fajardo and Solarte employed a method based on the Kubelka-Munk model [14] that measures diffuse transmission and reflection to determine the optical properties of cow's milk, specifically the absorption and diffusion coefficients. This highlights how optical properties, such as scattering and absorption coefficients, provide valuable insights into the morphological and biochemical composition of various materials, thus emphasizing the importance of separating them.

Various optical techniques are currently being explored to obtain different parameters that represent material conditions. One such technique is diffuse reflectance spectroscopy [15]-[18], which analyzes the light spectrum after reflection to derive the absorption and scattering properties of matter. However, it is worth noting that measurements of molar extinction coefficients are based on Beer-Lambert's law, which describes light attenuation from ballistic photons in a homogeneous medium. These measurements remain valid when particle density is low, and the path length of photons in the probed medium is short [19].

In dense or optically thick media, such as the dense region of a jet, biological tissues, or optically turbid liquid media, a large quantity of photons undergoes multiple scattering events. The contribution of these multiply scattered photons becomes significant, obscuring that of ballistic photons and constituting stray light that must be removed [19]. Under these conditions, the classical method of optical

spectroscopy is difficult to apply, although it is typically preferred for determining the optical properties of various compounds via the Beer-Lambert-Bouguer law. However, these measurements are no longer valid in optically dense media.

Due to the limitations of optical spectroscopy in optically dense media, a relatively new approach based on structured illumination has been developed [19]. This technique, known as SLIPI (Structured Illumination Planar Imaging), employs a spatially modulated laser sheet to pass through the dense medium under study. The light pattern formed within the medium is captured and processed to eliminate multiply scattered photons, significantly improving image contrast [20]. After removing the stray light, the optical density can be calculated, resulting in an exponential decay of intensity as the light passes through the sample [21].

This approach has been successfully used in 3D imaging for characterizing scattering media, determining molar extinction coefficients in turbid media [22], and classifying various types of coffee [23]. It has also proven to be a viable alternative for obtaining extinction coefficients in dense media where absorption spectrophotometry fails [24] and for diagnosing oils in power transformers, offering advantages over conventional monitoring methods like Interfacial Tension Turbidity (IFT), Dissolved Decay Products (DDP), and absorption spectrophotometry [25] [26].

In this article, we develop a new technique for independently calculating the absorption and scattering coefficients solely from single-phase SLIPI measurements. The proposed method involves synchronous detection alternated by using the Kubelka-Munk coefficients for scattering (S) and absorption (K) to determine the diffusion and absorption coefficients of an isotropic medium, primarily scattering or absorbing, such as milk and coffee. Specifically, the SLIPI method captures a modulated light sheet passing through the sample. The contribution of multiple light intensities is then removed during post-processing, producing an exponential intensity decay as light penetrates the sample. By fitting a curve to this decay and applying Beer-Lambert's law, we obtain the extinction and transmission coefficients of the sampled liquid [24].

Consequently, we can say that the SLIPI technique allows us to calculate the extinction coefficient, which is the sum of the absorption coefficient and the scattering coefficient. From SLIPI measurements and this equation, we derive another equation with two unknowns whose resolution yields multiple solutions. Using the Kubelka-Munk equations here enables us to develop additional equations useful for our experimental setup. These equations, collectively, provide more than one solution to separate the absorption and scattering coefficients of the various milk and coffee solutions selected for this study.

2. Materials and Methods

2.1. Sample Preparation

For the sample preparation, the coffee and milk solutions have been chosen. The former for their specific scattering feature and the latter for their special absorbing

feature. The solutions have been obtained according to the protocol described in [24] and summarized in Table 1 and Table 2. The photographs of the samples are presented in Figure 1 and Figure 2.

Table 1. Coffee sample preparation process.

Solutions	Coffee dilutions	Concentrations
1	m1 = 6 g of coffee dissolved in $V1$ = 450 ml of distilled water	$C1 = m1/V1$
2	$V2$ = 67.5 ml of solution 1 + 7.5 ml of distilled water	$C2 = 0.9 \times C1$
3	$V3$ = 60.0 ml of solution 1 + 15.0 ml of distilled water	$C3 = 0.8 \times C1$
4	$V4$ = 52.5 ml of solution 1 + 22.5 ml of distilled water	$C4 = 0.7 \times C1$
5	$V5$ = 45.0 ml of solution 1 + 30.0 ml of distilled water	$C5 = 0.6 \times C1$
6	$V6$ = 37.5 ml of solution 1 + 37.5 ml of distilled water	$C6 = 0.5 \times C1$
7	$V7$ = 30.0 ml of solution 1 + 45.0 ml of distilled water	$C7 = 0.4 \times C1$
8	$V8$ = 22.5 ml of solution 1 + 52.5 ml of distilled water	$C8 = 0.3 \times C1$
9	$V9$ = 15.0 ml of solution 1 + 60.0 ml of distilled water	$C9 = 0.2 \times C1$
10	$V10$ = 7.5 ml of solution 1 + 67.5 ml of distilled water	$C10 = 0.1 \times C1$

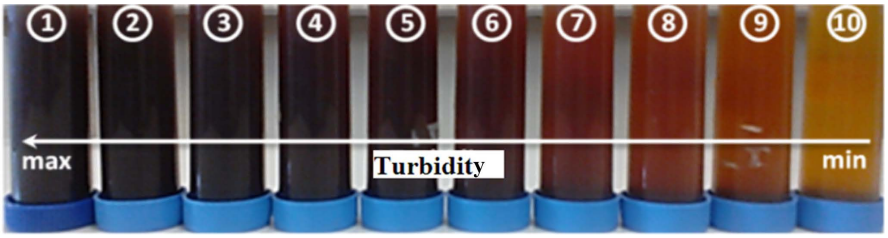

Figure 1. Photograph of coffee solutions samples classified from right to left according to the increasing order of turbidity.

Table 2. Milk sample preparation process.

Solutions	Milk dilutions	Concentrations
1	$V1$ = 5 ml of milk + 495 ml of distilled water	$C1$
2	$V2$ = 67.5 ml of solution 1 + 7.5 ml of distilled water	$C2 = 0.9 \times C1$
3	$V3$ = 60.0 ml of solution 1 + 15.0 ml of distilled water	$C3 = 0.8 \times C1$
4	$V4$ = 52.5 ml of solution 1 + 22.5 ml of distilled water	$C4 = 0.7 \times C1$
5	$V5$ = 45.0 ml of solution 1 + 30.0 ml of distilled water	$C5 = 0.6 \times C1$
6	$V6$ = 37.5 ml of solution 1 + 37.5 ml of distilled water	$C6 = 0.5 \times C1$
7	$V7$ = 30.0 ml of solution 1 + 45.0 ml of distilled water	$C7 = 0.4 \times C1$
8	$V8$ = 22.5 ml of solution 1 + 52.5 ml of distilled water	$C8 = 0.3 \times C1$
9	$V9$ = 15.0 ml of solution 1 + 60.0 ml of distilled water	$C9 = 0.2 \times C1$
10	$V10$ = 7.5 ml of solution 1 + 67.5 ml of distilled water	$C10 = 0.1 \times C1$

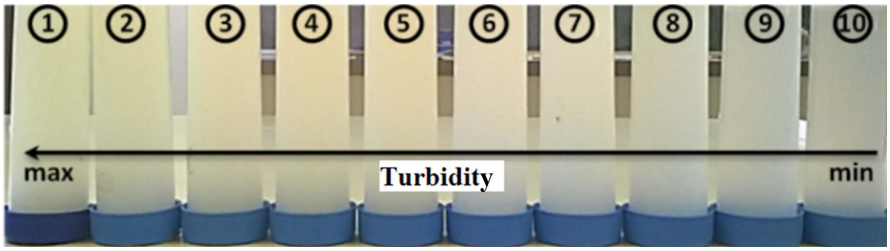

Figure 2. Photograph of milk solutions samples classified from right to left according to the increasing order of turbidity.

2.2. SLIPI-1p

In this section the SLIPI-1p approach is briefly described in sections. The details can be found in [27] and [28].

2.2.1. Experimental Device and Image Acquisition

A 450 nm or 638 nm continuous wave (CW) laser beam is used as the illumination source. The incident wave intensity is adjusted by using a density wheel in order to optimize the signal-to-noise ratio while avoiding saturation. Then, the beam is magnified by a factor of 10 by using a telescope device that is made with a pair of positive spherical lenses. An aperture is used to select the central part of the beam where the spatial intensity profile is quite homogeneous. A positive cylindrical lens with a focal length of 200 mm is used to create the sheet of laser light in the basin (L: 40 mm, l: 20 mm and h: 80 mm). To spatially modulate this sheet of laser light, a 2 lines/mm Ronchi grating is directly attached to the basin. This limits bad effects caused by near-field diffraction, known as the Talbot effect. A camera whose field of view direction is 90˚ with the light propagation direction is used to

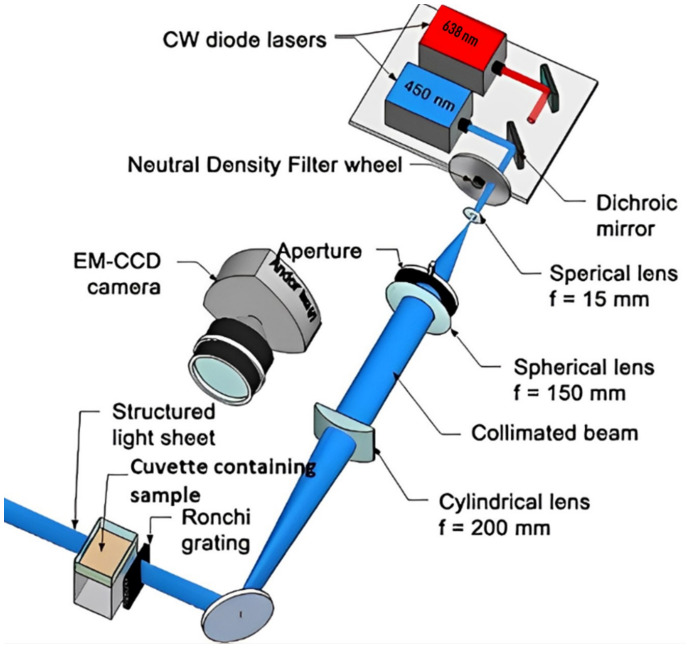

Figure 3. SLIPI-1p experimental device.

capture the images. It is an Andor brand Luca (r) CCD camera, with 14-bit electron multiplication. The final image is the result of accumulating more than 100 images to a single frame. The exposure time is between 0.001 and 0.1 seconds to optimize the dynamic range. The use of a Ronchi grating with 2 lp/mm is justified by its ability, in our experimental case, to spatially modulate light by generating a periodic pattern of dark and light bands across the sample with a relatively low spatial frequency (0.5 mm between each line), which is suitable for our study materials, such as milk and also for our camera. Indeed, the cut off frequency of the camera is over the spatial frequency of the Ronchi grating. **Figure 3** presents a diagram of the experimental device.

2.2.2. Data Processing and the Extinction Coefficient Extraction

The SLIPI approach used in this study relies on an analysis tool known as synchronous detection [29]. Synchronous detection, or 'lock-in amplifier,' is a common instrument used to address signal-to-noise ratio issues in research institutes and laboratories. It is a very powerful tool where signals of interest can be detected even if they are smaller than the accompanying noise signals. The lock-in amplifier is also used to detect and measure very small AC signals down to nano-volts or less, where noise remains a problem [30]. Synchronous detection is most often associated with the analysis of temporally varying signals, but it also works well for spatially modulated signals. To explain the principle of synchronous detection, let's consider a 1D signal, $I(x)$, with a superimposed periodic variation of amplitude I_s in space:

$$I(x) = I_s \sin(2\pi\vartheta x + \varphi) + I_{MS} \tag{1}$$

where I_s is the modulated light with a ballistic photonic signature; ϑ is the spatial frequency (mm^{-1}) of the modulation, and φ is the spatial phase, which is unknown. The term I_{MS} represents any undesirable non-modulated intensity contribution also detected, such as multiple light scattering or any other surrounding light sources. The goal of synchronous detection analysis is to extract I_s and reject I_{MS}. To achieve this, the signal (x) is multiplied by two reference signals R_1 and R_2, which are computationally generated with a relative phase shift of $\pi/2$:

$$R_1(x) = \sin(2\pi\vartheta x) \tag{2}$$

$$R_2(x) = \cos(2\pi\vartheta x) \tag{3}$$

By multiplying (x) by these reference signals, I_1 and I_2 are obtained.

$$I_1(x) = \frac{1}{2} I_S \left(\cos(\varphi) - \cos(4\pi\vartheta x + \varphi)\right) + I_{MS} \sin(2\pi\vartheta x) \tag{4}$$

$$I_2(x) = \frac{1}{2} I_S \left(\sin(\varphi) + \sin(4\pi\vartheta x + \varphi)\right) + I_{MS} \cos(2\pi\vartheta x) \tag{5}$$

The frequency analysis of I_1 and I_2 reveals three components: (1) a non-modulated component, (2) a component modulated at 2ϑ, and (3) another component modulated at ϑ. The last two components can be removed using a low-

pass filter in the Fourier domain, with a cutoff frequency below ϑ, resulting in the following expressions

$$\tilde{I}_1(x) = \frac{1}{2}\tilde{I}_S \cos(\varphi) \tag{6}$$

$$\tilde{I}_2(x) = \frac{1}{2}\tilde{I}_S \sin(\varphi) \tag{7}$$

where the tilde indicates that frequency filtering has been applied. From these, the SLIPI-1p image $\tilde{I}_S$ can finally be extracted by calculating:

$$\tilde{I}_S = 2\sqrt{\tilde{I}_1^2 + \tilde{I}_2^2} \tag{8}$$

An illustration of the SLIPI-1p process is shown in **Figure 4**. The example displays the signal from a structured laser light sheet, with effective sections extracted from two different depths, marked as A and B. A decrease in amplitude is observed from column A to column B. The 1D Fourier transforms of curves A and B show a reduction in the strength of the first-order peak (modulation frequency). This frequency is then isolated using frequency filtering (red zone) after applying the synchronous detection algorithm.

Finally, the exponential decay is revealed, as indicated in the SLIPI image and the corresponding I_s curve.

From a modulated image, the modulation amplitude is extracted using Equation (8). The modulated component, I_s, corresponds to the simple light diffusion that decreases exponentially with distance. By applying an exponential fit to I_s, the extinction coefficient μ_e is directly extracted as indicated by the Beer-Lambert-Bouguer law, which states that, assuming a collimated beam of a single wavelength traverses a uniform medium, the transmittance T is given by:

$$T = \frac{I_t}{I_0} = \mathrm{e}^{-\mu_e L} = \mathrm{e}^{-OD} \tag{9}$$

with T corresponding to the transmittance, which is a measure of light attenuation along the distance L. I_0 represents the incident light measured using a "blank" reference cuvette containing only the solvent. Then, I_t is the transmitted light, measured considering the solvent-solute mixture. Finally, μ_e is the extinction coefficient and OD is the optical path length.

The extinction coefficient μ_e is the sum of the absorption coefficient μ_a and the scattering coefficient μ_s showed in the Equation (10).

$$\mu_e = \mu_a + \mu_s \tag{10}$$

The absorption μ_a and diffusion μ_s coefficients are mixed in the extinction coefficient by a sum. In this study we would like to separate them, it means calculate both coefficients by only the use of SLIPI measurement.

A simple way to achieve it is to find another equation with the same unknown parameters μ_a and μ_s to have a system of two equation with two unknown parameters. That would permit to obtain μ_a and μ_s with simple calculation. In the following we obtain this second equation from the relations of the Kubeka-Munk theory.

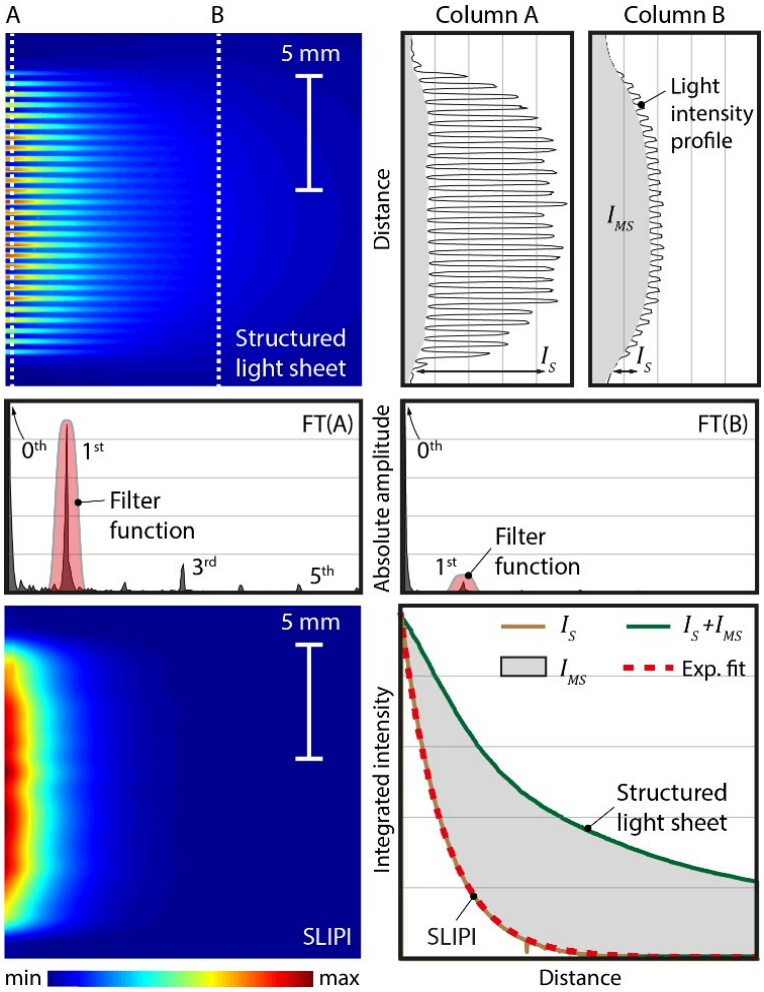

Figure 4. Principle of the SLIPI processing method. A first row (I) presents an original image obtained with the SLIPI set-up and the plot of the intensity at two different deeps A and B in the sample which clearly shows that the contributions of I_s are the periodic peaks. The second row (II) illustrates the reason of choosing the first harmonic as cut off frequency to filter the signal. The last row (III) presents the final SLIPI image and the comparison of the exponential decay plots obtained from SLIPI and original images to show the improvement achieved by the technique.

2.3. Kubelka-Munk theory and relationships

The Kubelka-Munk model is a two-flux radiative transfer model that predicts the reflectance and transmittance of a homogeneous absorbing and scattering layer illuminated by Lambertian radiation. We consider a thin substratum of depth dz and we respectively denote i and j as the downward and upward facing Lambertian fluxes (see Figure 5). It is assumed that the variations of these fluxes are due to absorption and scattering.

K and S are the Kubelka-Munk coefficients associated respectively with the absorption and scattering of the medium per length unit. As it gets into the layer of depth dz, the downward flow i decreases by the amount $(K+S)i\mathrm{d}z$ due to

absorption and scattering, and it further increases by the amount $Sidz$ due to the backscattering loss of the upward flow j. The same reasoning on the upward flow j leads to the following system of differential equations which can be solved in several ways, for example by using the Laplace transformation [31] or the matrix exponential method [32]:

$$\frac{\mathrm{d}i}{\mathrm{d}z} = -(K+S)i + Sj \tag{11}$$

$$\frac{\mathrm{d}j}{\mathrm{d}z} = -Si + (K+S)j \tag{12}$$

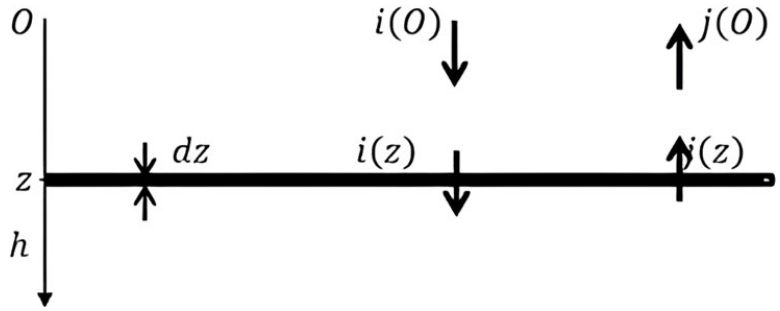

Figure 5. Upward and downward flow through a thin substratum of depth dz.

Indeed, the relationship between KubelKa-Munk coefficients and transport coefficients has been examined by several researchers previously. They used the radiative transfer equation as a starting point [33]-[35]. In this case the expression for the KubelKa-Munk absorption coefficient K is given by the Equation (13) as a function of absorption coefficient μ_a [34] [36]-[38].

$$K = 2\mu_a \tag{13}$$

On the other hand, the KubelKa-Munk scattering coefficient relation is obtained by a semi-empirical approach. By using this approach, the relation is derived for the case of incident collimated light. Thus, in isotropic domain, Klier and Gate have shown that the scattering coefficient of KubelKa-Munk noted S can be expressed as a function of the scattering coefficient μ_s by the following expression:

$$S = \frac{3}{4}\mu_s \tag{14}$$

With the local optical characteristics K and S assumed to be independent of the medium depth, Kubelka-Munk defines the following parameters [34] [36]-[39]:

$$\alpha = \sqrt{K(K+2S)} \tag{15}$$

$$\beta = \sqrt{\frac{K}{K+2S}} \tag{16}$$

We note, in addition, that the calculation of the coefficients has been standardized (ISO standard) following the method proposed by Kubelka-Munk [40]. Also it should be said that the Kubelka-Munk theory is one of the theories based on the

scattering approximation and is widely used to obtain the optical properties from the measured reflectance spectra. Today this theory is widely used in the fields of multispectral imaging or structured illumination [12] to measure the optical properties of certain media such as turbid media. Moreover, the advantage of this theory is that it provides simple analytical expressions to obtain the optical parameters from the measured total reflectance or transmittance of a diffusive medium [37]. However, the conditions for the application of the Kubelka-Munk theory require a diffuse or collimated, monochromatic and isotropic light source. Also the sample must be homogeneously and isotropically absorbing or scattering. This corresponds perfectly to the SLIPI-1p technique. Thus we can say that the conditions of these equations use are applicable to SLIPI-1p.

2.4. Technique for Calculating Absorption Coefficient and Diffusion Coefficient

Beer Lambert's law exploited by the SLIPI-1p method allows the determination of the extinction coefficient μ_e from the measurements made by transmittance. However, let us notify here that our medium being isotropic with a detection angle of π/2, we obtain an anisotropy factor $g = 0$ which leads to an equality between the reduced scattering coefficient μ_s' and the scattering coefficient μ_s as suggested by the Equation (17) from [36].

$$\mu_s' = \mu_s (1 - g) \tag{17}$$

The relationship between the extinction coefficient μ_e, the absorption coefficient μ_a and the scattering coefficient μ_s given by the Equation (10) does not allow the calculation of the other two coefficients [41]. We end up with an equation with two unknowns. A simple calculation would consist in finding a second equation with the same unknowns. The contribution of KubelKa-Munk's relations in this study is therefore this second equation that allows us to calculate easily the absorption coefficient μ_a and the scattering coefficient μ_s. Therefore, the relationships between the Kubelka-Munk coefficients, μ_a and μ_s are introduced [34] [36]-[38]. In the case of an isotropic medium, these relations are given by the Equations (13) and (14) where K is the fraction of the flux that is absorbed and S is the fraction of the flux that is scattered.

Substituting the Equations (13) and (14) into the Equations (15) and (16), we have the expressions for α and β as a function of μ_a and μ_s given by the Equations (18) and (19).

$$\alpha = \sqrt{\mu_a (4\mu_a + 3\mu_s)} \tag{18}$$

$$\beta = \sqrt{\frac{4\mu_a}{4\mu_a + 3\mu_s}} \tag{19}$$

Thus

$$\frac{\alpha}{\beta} = \frac{4\mu_a + 3\mu_s}{2} \tag{20}$$

$$\alpha \cdot \beta = 2\mu_a \tag{21}$$

From the Equation (10), we can derive the relation

$$4\mu_a + 3\mu_s = \mu_a + 3\mu_e \tag{22}$$

This relation is replaced in the Equations (19) and (20) to obtain the expression of α as a function of β, μ_a and μ_e given by the Equation (21).

$$\alpha = \frac{\beta\left(\mu_a + 3\mu_e\right)}{2} \tag{23}$$

The expression for α thus obtained is replaced in the Equation (20) and an expression for μ_a as a function of β and μ_e given by the Equation (11) is derived.

$$\mu_a = \frac{3\beta^2}{4-\beta^2}\mu_e \tag{24}$$

The Equation (1) and (11) are then used to obtain the Equation (12) which is the expression for μ_s as a function of β and μ_e.

$$\mu_s = \frac{4\left(1-\beta^2\right)}{4-\beta^2}\mu_e \tag{25}$$

The expressions for μ_a and μ_s are obtained as a function of μ_e which is the measurement that is therefore known and β as an unknown parameter. The idea is to find an estimate of the parameter β. It is easy to notice that we obtain a function $g(\beta)$ that is given by the Equation (24) when we perform the calculation $\mu_s - \mu_a$.

$$g(\beta) = \frac{4-7\beta^2}{4-\beta^2}\mu_e \tag{26}$$

The variations of this function combined with $\beta \geq 0$; $-\mu_e \leq \mu_s - \mu_a \leq \mu_e$ and impose a value of β between 0 and 1 with:

- $\beta \in \left[0, \frac{2}{\sqrt{7}}\right[$, $\mu_s > \mu_a$, so, this is the range of β values for more scattering media;
- $\beta \in \left]\frac{2}{\sqrt{7}}, 1\right[$, $\mu_s < \mu_a$, so, this is the range of β values for more absorbent media.

The use of the relations between the KubelKa-Munk coefficients and the radiative transfer coefficients of the light imposes the case of a preponderant diffusion. We can therefore write:

$$\frac{\mu_a}{\mu_s} = \frac{3\beta^2}{4\left(1-\beta^2\right)} \ll 1 \approx \varepsilon \tag{27}$$

ε the ratio of μ_a to μ_s is a very small value in terms of which we estimate from (27)

$$\beta \leq \sqrt{\frac{4\varepsilon}{3+4\varepsilon}} \tag{28}$$

The calculation of μ_a and μ_s required to know the value of β. A direct calculation is not possible but β can be estimated as suggested by the inequation (28). Therefore, the estimated value of β only depend on the accuracy of the estimation of ε. In a context of mathematical situations called precision or tolerance, ε must be chosen as a threshold to minimize or compare the two physical parameters obtained [42]-[44] and its current value is 10^{-3} which leads to $\beta \approx 0.036$. This value of ε can be adjusted according to the accuracy requirements and the characteristics of the problem. In the case of this study, we choose to directly ensure of the accuracy of β. Our approach was to calculate β from the Equation (27) using the value of μ_a and μ_s found in the literature for the media used it means milk and coffee. The value found is of the order of 0.03 with respect to milk of a strongly scattering nature [45]-[49] that permit to confirm $\beta \approx 0.036$.

We can overlook the fact that the relationships between the KubelKa-Munk coefficients and the radiative transfer coefficients are largely obtained in the case of predominantly diffusion and rigorously obtain $\beta \approx 0.999$ for the calculation of μ_a and μ_s for highly absorbing solutions such as coffee.

3. Results

We developed an analytical method for separately evaluating the diffusion coefficient and the absorption coefficient from measurements of the extinction coefficient at 450 nm and 638 nm. We applied this technique to solutions of milk and coffee, two media known for their high scattering and absorption capacities respectively. Measurements carried out on the milk and coffee samples using the SLIPI-1p method described in the previous sections were used to obtain the extinction coefficients. Equations (24) and (25) are then used to calculate the absorption and diffusion coefficients. The different values (mm^{-1}) obtained at 450 nm and 638 nm are given in **Table 3** for the milk solutions and **Table 4** for the coffee solutions.

Table 3. Values of absorption, scattering and extinction coefficients of milk solutions.

Milk Solutions	Coefficients at 450 nm			Coefficients at 638 nm		
	μ_e	μ_s	μ_a	μ_e	μ_s	μ_a
1	2.0467	2.0447	0.0020	1.1431	1.1420	0.0011
2	1.8870	1.8852	0.0018	1.0455	1.0445	0.0010
3	1.7677	1.7660	0.0017	0.9378	0.9369	0.0009
4	1.5883	1.5868	0.0015	0.8353	0.8345	0.0008
5	1.3626	1.3613	0.0013	0.7301	0.7294	0.0007
6	1.1676	1.1665	0.0011	0.6103	0.6097	0.0006
7	0.9502	0.9493	0.0009	0.5018	0.5012	0.0005
8	0.7125	0.7118	0.0007	0.3769	0.3765	0.0004
9	0.5032	0.5029	0.0005	0.2614	0.2611	0.0003
10	0.2561	0.2558	0.0003	0.1366	0.1365	0.0001

The results show significant variability in the extinction, absorption and diffusion coefficients as a function of the characteristics of the media studied. Table 3 and Table 4 show a progressive decrease in the scattering and absorption coefficients with increasing dilution of the milk and coffee solutions at both 450 nm and 638 nm. These variations are consistent with expectations, given that the concentration of dispersing particles in the milk solutions directly influences these coefficients and is also indicative of the optical behaviour of coffee, a predominantly absorbing medium.

Table 4. Values of absorption, scattering and extinction coefficients of coffee solutions.

Coffee Solutions	Coefficients at 450 nm			Coefficients at 638 nm		
	μ_e	μ_s	μ_a	μ_e	μ_s	μ_a
1	2.1503	0.0057	2.1446	0.8374	0.0022	0.8352
2	1.9539	0.0052	1.9487	0.7201	0.0019	0.7182
3	1.7526	0.0047	1.7479	0.6511	0.0017	0.6423
4	1.5453	0.0041	1.5412	0.5640	0.0015	0.5629
5	1.3124	0.0035	1.3089	0.4803	0.0013	0.4791
6	1.1018	0.0029	1.0989	0.4061	0.0011	0.4049
7	0.8202	0.0022	0.8180	0.2996	0.0008	0.2988
8	0.6504	0.0017	0.6487	0.2403	0.0006	0.2397
9	0.4213	0.0011	0.4202	0.146	0.0004	0.1456
10	0.1890	0.0005	0.1885	0.0701	0.0002	0.0699

4. Discussion

The results obtained for milk and coffee solutions, presented in Table 3 and Table 4, provide essential information on the optical properties of these media. This study highlights the marked differences between the behaviour of a scattering medium (milk) and an absorbing medium (coffee), which enriches our understanding of light-matter interactions.

Analysis of the absorption and scattering coefficients obtained at 450 nm shows that the scattering values measured for milk, corresponding to reduced scattering coefficients, are close to those reported in previous studies [46]-[49], although distinct. On the other hand, the absorption coefficients are slightly higher than those in the literature, a difference that can be attributed to the quality of the milk used, its manufacturing process (around 9.6% fat) and the sampling conditions. These variations can also be influenced by the wavelength, which affects the absorption and diffusion coefficients.

The measured coefficients show distinct behaviours depending on the type of solution. For milk, the high scattering values at 450 nm indicate strong scattering due to the presence of dispersed particles. Conversely, the results for coffee reveal much higher absorption coefficients, which is consistent with previous studies

showing that pigment rich media such as coffee absorb light efficiently in the blue region [50]. With increasing dilution, there is a progressive decrease in the extinction, absorption and scattering coefficients in both media. For milk solutions, this decrease is linked to a reduction in the concentration of scattering particles, while for coffee it is explained by a decrease in the quantity of absorbing chromophores. As Tuchin [51] points out, optically turbid media such as milk and coffee show predictable behaviour as a function of their component concentration, underlining the importance of this concentration in the analysis of optical properties.

At higher wavelengths, such as 638 nm, the measured coefficients are significantly lower, reflecting less interaction of red light with the chromophoric components of coffee. This is consistent with previous studies on coffee extracts [52] and illustrates the variability of light interactions as a function of wavelength, as also shown by Nascimento *et al.* [53], with chromophores absorbing specifically at certain wavelengths.

The method developed in this study enables the determination of the absorption coefficient (μ_a) and scattering coefficient (μ_s) from simple measurements of the extinction coefficient (μ_e). These two coefficients, initially unknowns in the equation, represent fundamental physical properties of the media studied. The absorption coefficient (μ_a) corresponds to the medium's intrinsic ability to absorb light, which depends on molecular characteristics and the chromophores present, as observed in coffee solutions. In contrast, the scattering coefficient (μ_s) reflects the extent of light scattering, influenced by the size, concentration, and distribution of suspended particles, as demonstrated in the case of milk.

Solving for these two coefficients adds significant value, as it provides a deeper understanding of each mechanism's contribution (absorption vs. scattering) to the overall extinction coefficient (μ_e). This distinction is crucial for analyzing media where one of these parameters may dominate, such as milk (high scattering) and coffee (high absorption). The ability to obtain separate values for μa and μs solely from μe represents a notable advancement over traditional methods, which generally require multiple complementary measurements to isolate each coefficient.

Thus, this study demonstrates that highly scattering and concentrated or absorbing and concentrated media can have their optical properties measured effectively. Eliminating the contributions of multiple scattering in the dense liquid medium under study allows for direct measurement of the absorption and scattering coefficients, unlike conventional techniques, giving the proposed method an advantage for future optical characterization studies.

5. Conclusions

This study presents a new method to independently calculate the absorption and diffusion coefficients of dense, highly absorbing or scattering liquid media, such as milk and coffee. Using a continuous-wave He-Ne laser beam at wavelengths of 450 nm and 638 nm, and applying a combination of the single-phase SLIPI

technique with Kubelka-Munk relations, we obtained consistent and conclusive results, demonstrating the effectiveness of this approach both experimentally and theoretically.

Our results emphasize the critical importance of wavelength in light-matter interactions for these media. This technique revealed distinct optical behaviors depending on the nature of the solutions and the wavelength, providing a precise insight into the mechanisms of absorption and diffusion. While our current method is limited to optically homogeneous media with high absorption or scattering properties, future research will aim to adapt and extend this technique to liquids exhibiting mixed optical properties, thereby enriching the possibilities for analysis.

The potential applications of this approach are promising, particularly in the field of food quality control, where it could help optimize production processes based on variations in optical properties. For example, in the coffee industry, an increase in the absorption coefficient could indicate changes in the quality of roasting or beans, directly influencing taste and aroma. In the dairy sector, distinct measurement of absorption and diffusion coefficients could be used to assess milk quality, highlighting changes related to the manufacturing or preservation process.

Furthermore, this study opens new perspectives for exploring absorption and diffusion phenomena in dense and anisotropic media, contributing to a better understanding of complex optical interactions. These advancements will not only refine our methods for a variety of media but also extend the scope of this technique to diverse sectors, in alignment with our broader research objectives.

Acknowledgments

The authors would like to thank the Head of the Département de Formation et de Recherche du Génie Electrique et Electronique at Institut National Polytechnique Felix Houphouët-Boigny for his encouragement and support. Special thanks go to the reviewers for their critical contribution.

Conflicts of Interest

The authors declare no conflicts of interest.

References

[1] Prasad, P.N. (2003) Introduction to Biophotonics. John Wiley & Sons. https://doi.org/10.1002/0471465380

[2] Durduran, T., Choe, R., Baker, W.B. and Yodh, A.G. (2010) Diffuse Optics for Tissue Monitoring and Tomography. *Reports on Progress in Physics*, **73**, Article 076701. https://doi.org/10.1088/0034-4885/73/7/076701

[3] Patterson, M.S., Wilson, B.C. and Wyman, D.R. (1991) The Propagation of Optical Radiation in Tissue I. Models of Radiation Transport and Their Application. *Lasers in Medical Science*, **6**, 155-168. https://doi.org/10.1007/bf02032543

[4] Star, W.M. (1997) Light Dosimetry *in vivo*. *Physics in Medicine and Biology*, **42**, 763-

787. https://doi.org/10.1088/0031-9155/42/5/003

[5] Davidson, S.R.H., Weersink, R.A., Haider, M.A., Gertner, M.R., Bogaards, A., Giewercer, D., *et al.* (2009) Treatment Planning and Dose Analysis for Interstitial Photodynamic Therapy of Prostate Cancer. *Physics in Medicine and Biology*, **54**, 2293-2313. https://doi.org/10.1088/0031-9155/54/8/003

[6] Moore, C.M., Mosse, C.A., Allen, C., Payne, H., Emberton, M. and Bown, S.G. (2011) Light Penetration in the Human Prostate: A Whole Prostate Clinical Study at 763 nm. *Journal of Biomedical Optics*, **16**, Article 015003. https://doi.org/10.1117/1.3528638

[7] Pantelides, M.L., Whitehurst, C., Moore, J.V., King, T.A. and Blacklock, N.J. (1990) Photodynamic Therapy for Localised Prostatic Cancer: Light Penetration in the Human Prostate Gland. *Journal of Urology*, **143**, 398-401. https://doi.org/10.1016/s0022-5347(17)39973-1

[8] Lin, A.J., Koike, M.A., Green, K.N., Kim, J.G., Mazhar, A., Rice, T.B., *et al.* (2011) Spatial Frequency Domain Imaging of Intrinsic Optical Property Contrast in a Mouse Model of Alzheimer's Disease. *Annals of Biomedical Engineering*, **39**, 1349-1357. https://doi.org/10.1007/s10439-011-0269-6

[9] Nguyen, T.T.A., Ramella-Roman, J.C., Moffatt, L.T., Ortiz, R.T., Jordan, M.H. and Shupp, J.W. (2013) Novel Application of a Spatial Frequency Domain Imaging System to Determine Signature Spectral Differences between Infected and Noninfected Burn Wounds. *Journal of Burn Care & Research*, **34**, 44-50. https://doi.org/10.1097/bcr.0b013e318269be30

[10] Johansson, A., Axelsson, J., Andersson-Engels, S. and Swartling, J. (2007) Realtime Light Dosimetry Software Tools for Interstitial Photodynamic Therapy of the Human Prostate. *Medical Physics*, **34**, 4309-4321. https://doi.org/10.1118/1.2790585

[11] Zaccanti, G., Del Bianco, S. and Martelli, F. (2003) Measurements of Optical Properties of High-Density Media. *Applied Optics*, **42**, 4023-4030. https://doi.org/10.1364/ao.42.004023

[12] Cuccia, D.J., Bevilacqua, F., Durkin, A.J., Ayers, F.R. and Tromberg, B.J. (2009) Quantitation and Mapping of Tissue Optical Properties Using Modulated Imaging. *Journal of Biomedical Optics*, **14**, Article 024012. https://doi.org/10.1117/1.3088140

[13] Lenz, A.J.M., Clemente, P., Climent, V., Lancis, J. and Tajahuerce, E. (2019) Imaging the Optical Properties of Turbid Media with Single-Pixel Detection Based on the Kubelka-Munk Model. *Optics Letters*, **44**, 4797-4800. https://doi.org/10.1364/ol.44.004797

[14] Kubelka, P. (1948) New Contributions to the Optics of Intensely Light-Scattering Materials Part I. *Journal of the Optical Society of America*, **38**, 448-457. https://doi.org/10.1364/josa.38.000448

[15] Murphy, B.W., Webster, R.J., Turlach, B.A., Quirk, C.J., Clay, C.D., Heenan, P.J., *et al.* (2005) Toward the Discrimination of Early Melanoma from Common and Dysplastic Nevus Using Fiber Optic Diffuse Reflectance Spectroscopy. *Journal of Biomedical Optics*, **10**, Article 064020. https://doi.org/10.1117/1.2135799

[16] Koenig, F., Larne, R., Enquist, H., McGovern, F.J., Schomacker, K.T., Kollias, N., *et al.* (1998) Spectroscopic Measurement of Diffuse Reflectance for Enhanced Detection of Bladder Carcinoma. *Urology*, **51**, 342-345. https://doi.org/10.1016/s0090-4295(97)00612-2

[17] Bigio, I.J., Bown, S.G., Briggs, G., Kelley, C., Lakhani, S., Pickard, D., *et al.* (2000) Diagnosis of Breast Cancer Using Elastic-Scattering Spectroscopy: Preliminary Clinical Results. *Journal of Biomedical Optics*, **5**, 221-228. https://doi.org/10.1117/1.429990

[18] Mourant, J.R., Bigio, I.J., Boyer, J., Conn, R.L., Johnson, T. and Shimada, T. (1995) Spectroscopic Diagnosis of Bladder Cancer with Elastic Light Scattering. *Lasers in Surgery and Medicine*, **17**, 350-357. https://doi.org/10.1002/lsm.1900170403

[19] Bergmann, F., Foschum, F., Zuber, R. and Kienle, A. (2020) Precise Determination of the Optical Properties of Turbid Media Using an Optimized Integrating Sphere and Advanced Monte Carlo Simulations. Part 2: Experiments. *Applied Optics*, **59**, 3216-3226. https://doi.org/10.1364/ao.385939

[20] Berrocal, E., Johnsson, J., Kristensson, E. and Aldén, M. (2012) Single Scattering Detection in Turbid Media Using Single-Phase Structured Illumination Filtering. *Journal of the European Optical Society-Rapid Publications*, **7**, Article No. 12015. https://doi.org/10.2971/jeos.2012.12015

[21] Kristensson, E., Bood, J., Alden, M., Nordström, E., Zhu, J., Huldt, S., *et al.* (2014) Stray Light Suppression in Spectroscopy Using Periodic Shadowing. *Optics Express*, **22**, 7711-7721. https://doi.org/10.1364/oe.22.007711

[22] Kristensson, E., Berrocal, E. and Aldén, M. (2012) Quantitative 3D Imaging of Scattering Media Using Structured Illumination and Computed Tomography. *Optics Express*, **20**, 14437-14450. https://doi.org/10.1364/oe.20.014437

[23] K. Bagui, O., A. Kaduki, K., Berrocal, E. and T. Zoueu, J. (2016) Structured Laser Illumination Planar Imaging Based Classification of Ground Coffee Using Multivariate Chemometric Analysis. *Applied Physics Research*, **8**, 32-44. https://doi.org/10.5539/apr.v8n3p32

[24] Regnima, G., Koffi, T., Bagui, O., Kouacou, A., Kristensson, E., Zoueu, J., *et al.* (2017) Quantitative Measurements of Turbid Liquids via Structured Laser Illumination Planar Imaging Where Absorption Spectrophotometry Fails. *Applied Optics*, **56**, 3929-3938. https://doi.org/10.1364/ao.56.003929

[25] Koffi, T., Kassi, K.S., Kone, G., N'Cho, J.S., Edoé, M., Bosson, J., *et al.* (2022) Using Structured Laser Illumination Planar Imaging (SLIPI) as a New Technique to Monitor the Degradation of Biodegradable Oils in Electrical Power Transformers. *IET Generation, Transmission & Distribution*, **16**, 2642-2653. https://doi.org/10.1049/gtd2.12480

[26] Regnima, G., Betié, A., Koffi, T., Bagui, O.K., Fofana, I., Kouacou, A., *et al.* (2018) Monitoring Power Transformers Oils Deterioration Using Structured Laser Illumination Planar Imaging. *Measurement*, **113**, 38-45. https://doi.org/10.1016/j.measurement.2017.08.019

[27] Kristensson, E. (2012) Structured Laser Illumination Planar Imaging-SLIPI: Applications for Spray Diagnostics. Doctoral Thesis, Department of Physics, Lund University.

[28] Berrocal, E., Kristensson, E., Richter, M., Linne, M. and Aldén, M. (2008) Application of Structured Illumination for Multiple Scattering Suppression in Planar Laser Imaging of Dense Sprays. *Optics Express*, **16**, 17870-17881. https://doi.org/10.1364/oe.16.017870

[29] Meade, M.L. (1982) Advances in Lock-in Amplifiers. *Journal of Physics E*: *Scientific Instruments*, **15**, 395-403. https://doi.org/10.1088/0022-3735/15/4/001

[30] Petricka, J. (2014) An Introduction to the Lock-IN Amplifier and a Mie Scattering Ex-periment. Gustavus Adolphus College PHY-305. https://advlabs.aapt.org/document/ServeFile.cfm?ID=14315&DocID=4675

[31] Hébert, M., Hersch, R.D. and Emmel, P. (2014) Fundamentals of Optics and Radiometry for Color Reproduction. In: Kriss, M., Ed., *Handbook of Digital Imaging*, Wiley, 1021-1077.

[32] Hébert, M. and Emmel, P. (2015) Two-Flux and Multiflux Matrix Models for Colored Surfaces. In: Kriss, M., Ed., Handbook of Digital Imaging, Wiley, 1233-1277.

[33] Brinkworth, B.J. (1972) Interpretation of the Kubelka-Munk Coefficients in Reflection Theory. *Applied Optics*, **11**, 1434-1435. https://doi.org/10.1364/ao.11.001434

[34] Gate, L.F. (1974) Comparison of the Photon Diffusion Model and Kubelka-Munk Equation with the Exact Solution of the Radiative Transport Equation. *Applied Optics*, **13**, 236-238. https://doi.org/10.1364/ao.13.000236

[35] Star, W.M., Marijnissen, J.P.A. and van Gemert, M.J.C. (1988) Light Dosimetry in Optical Phantoms and in Tissues: I. Multiple Flux and Transport Theory. *Physics in Medicine and Biology*, **33**, 437-454. https://doi.org/10.1088/0031-9155/33/4/004

[36] Roy, A., Ramasubramaniam, R. and Gaonkar, H.A. (2012) Empirical Relationship between Kubelka-Munk and Radiative Transfer Coefficients for Extracting Optical Parameters of Tissues in Diffusive and Nondiffusive Regimes. *Journal of Biomedical Optics*, **17**, Article 115006. https://doi.org/10.1117/1.jbo.17.11.115006

[37] Klier, K. (1972) Absorption and Scattering in Plane Parallel Turbid Media. *Journal of the Optical Society of America*, **62**, 882-885. https://doi.org/10.1364/josa.62.000882

[38] Thennadil, S.N. (2008) Relationship between the Kubelka-Munk Scattering and Radiative Transfer Coefficients. *Journal of the Optical Society of America A*, **25**, 1480-1485. https://doi.org/10.1364/josaa.25.001480

[39] Simonot, L., Thoury, M. and Delaney, J. (2011) Extension of the Kubelka-Munk Theory for Fluorescent Turbid Media to a Nonopaque Layer on a Background. *Journal of the Optical Society of America A*, **28**, 1349-1457. https://doi.org/10.1364/josaa.28.001349

[40] ISO 9416: 2017(en) Paper—Determination of Light Scattering and Absorption Coefficients (Using Kubelka-Munk Theory). https://www.iso.org/obp/ui/#iso:std:iso:9416:ed-3:v1:en

[41] Steelman, Z.A., Ho, D.S., Chu, K.K. and Wax, A. (2019) Light-Scattering Methods for Tissue Diagnosis. *Optica*, **6**, 479-489. https://doi.org/10.1364/optica.6.000479

[42] Ralph, E. (2005) Numerical Methods for Engineers and Scientists. Wiley.

[43] Kincaid, D., Cheney, W. (2002) Numerical Analysis: Mathematics of Scientific Computing. American Mathematical Society.

[44] Burden, R. L., Faires, J. D. (2010) Numerical Analysis. Cengage Learning.

[45] Sassaroli, A., Blumetti, C., Martelli, F., Alianelli, L., Contini, D., Ismaelli, A., *et al.* (1998) Monte Carlo Procedure for Investigating Light Propagation and Imaging of Highly Scattering Media. *Applied Optics*, **37**, 7392-7400. https://doi.org/10.1364/ao.37.007392

[46] Michielsen, K., Raedt, H.D., Przeslawski, J. and Garcia, N. (1998) Computer Simulation of Time-Resolved Optical Imaging of Objects Hidden in Turbid Media. *Physics Reports*, **304**, 89-144. https://doi.org/10.1016/s0370-1573(98)00023-4

[47] Das, C., Trivedi, A., Mitra, K. and Vo-Dinh, T. (2003) Experimental and Numerical Analysis of Short-Pulse Laser Interaction with Tissue Phantoms Containing Inhomogeneities. *Applied Optics*, **42**, 5173-5180. https://doi.org/10.1364/ao.42.005173

[48] Gwamuri, J., Gholap, A.V., Shartir, T.S.M. and Bauh-Bassuah, P.K. (2014) Investigating Light Propagation in Turbid Media by Evaluating Optical Properties of Phantom Tissues. https://appropriatetech.net/?q=content/2nd-icat-energy-physics

[49] Mohamed, T.S. (2000) Investigating Laser Light Interaction by Studying Photon

Propagation and Optical Imaging through a Medium with Embedded Inhomogeneities. Thèse de doctorat, Université du Cap-Vert.

[50] Pérez, A., Gómez-Alonso, S., García-Viguera, C. (2018) Influence of Pigments on the Optical Properties of Coffee. *Journal of Agricultural and Food Chemistry*, **66**, 2430-2436.

[51] Tuchin, V.V. (2018) Tissue Optics: Light Scattering Methods and Instruments for Medical Diagnostics, 3e Édition, SPIE Press.

[52] Khan, M.I., Zia-Ul-Haq, M., Ullah, F. and Bhatti, H.N. (2016) Optical Properties of Coffee Extracts: Implications for Quality Assessment. *Food Research International*, **89**, 559-565.

[53] Nascimento, D.M., Dias, C.T., Cordeiro, A.M. and Rodrigues, J.F. (2019) Light Absorption in Beverages: Understanding the Effects of Composition and Processing. *Journal of Food Science*, **84**, 1162-1172.